Appendix files – Table of contents

Appendix Figures:

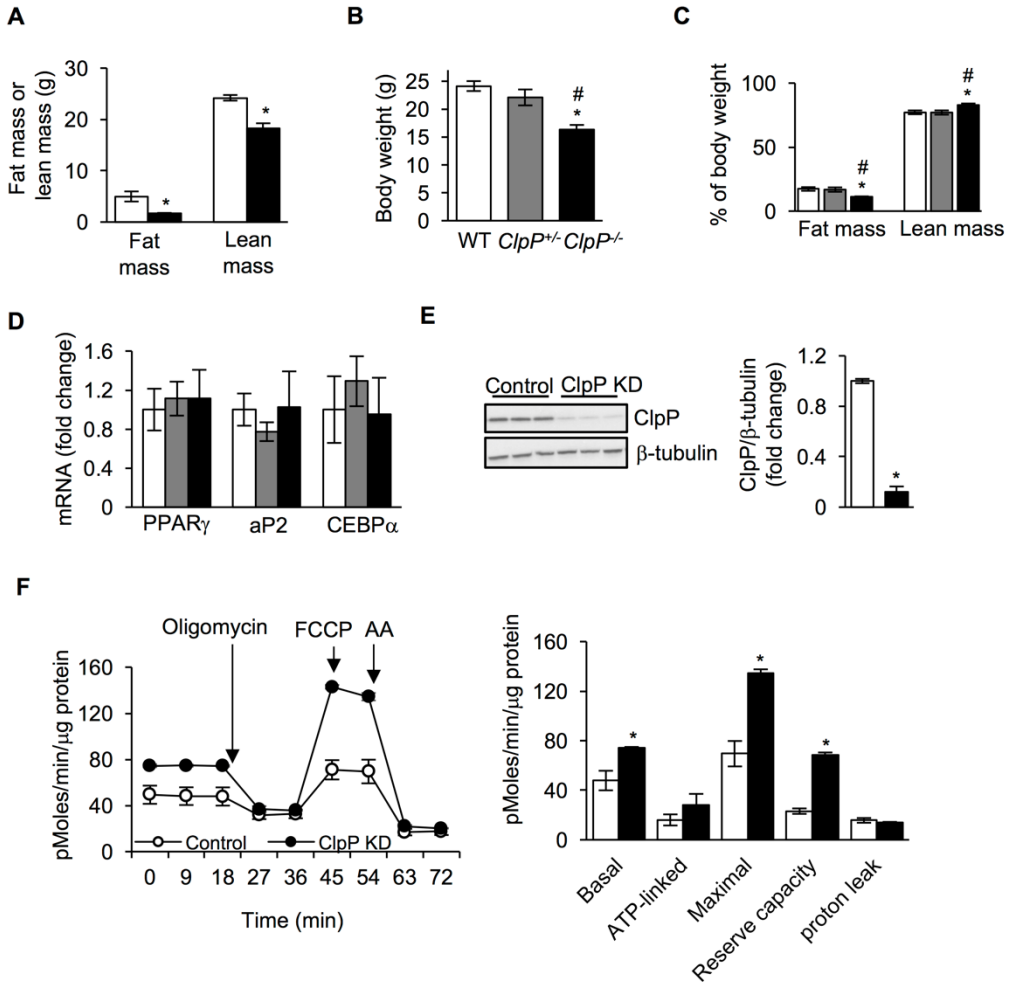

Appendix Figure S1. *ClpP*$^{-/-}$ mice have reduced adiposity and elevated respiration in WAT.

(A) Fat mass and lean mass in WT and *ClpP*$^{-/-}$ male mice, assessed by QMR imaging (n = 8-10).
(B) Body weights of WT, *ClpP*$^{+/-}$ and *ClpP*$^{-/-}$ female mice fed *ad libitum* at 5 months of age (n = 8).
(C) Fat mass and lean mass of female WT, *ClpP*$^{+/-}$ and *ClpP*$^{-/-}$ mice, assessed by QMR imaging and normalized to body weight (n = 8).
(D) Transcript levels of PPARγ, aP2 and CEBPα in gWAT of WT, *ClpP*$^{+/-}$ and *ClpP*$^{-/-}$ male mice fed *ad libitum* at 5 months of age (n = 6).
(E) Westernblots showing protein expression of ClpP and β-tubulin in differentiated 3T3-L1 control or ClpP knockdown (KD) adipocytes (left panel) (n = 3). Quantification of ClpP normalized to β-tubulin is shown in the right panel.
(F) Cellular bioenergetics in differentiated 3T3-L1 control or ClpP KD adipocytes measured using the Seahorse Bioscience XF24 Extracellular Flux Analyzer mitostress assay (left panel). Graphical representation of the obtained values normalized to protein concentration per well (right panel). (n = 3). Data represents mean±SEM from three independent experiments.

Data information: (A-F) Bars represent mean ± SEM. (ANOVA, *WT/Control vs *ClpP*$^{-/-}$/ClpPKD; #*ClpP*$^{+/-}$ vs *ClpP*$^{-/-}$. */#p<0.05). WT/Control-white bars, *ClpP*$^{+/-}$-grey bars, *ClpP*$^{-/-}$/ClpPKD-black bars.

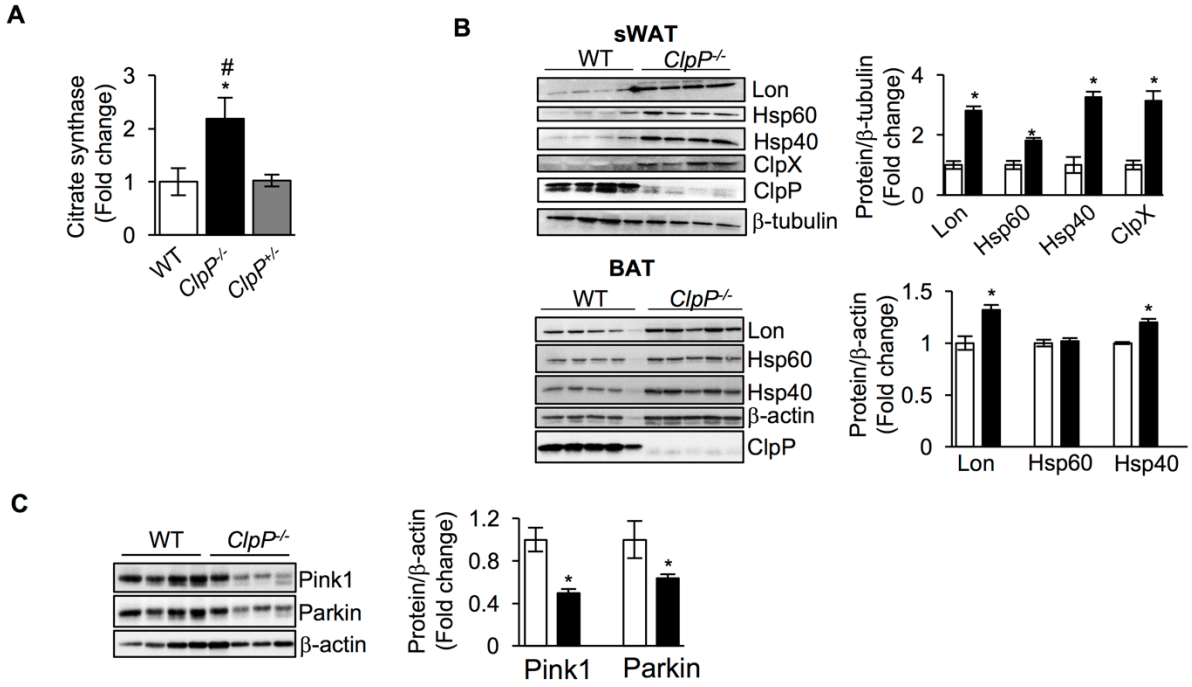

Appendix Figure S2. Markers of mitochondrial biogenesis mitochondrial chaperones, and mitochondrial fission/fusion regulator OPA1 are elevated in gWAT of *ClpP*$^{-/-}$ mice.

(A) Quantification of protein levels of citrate synthase in gWAT of WT, *ClpP*$^{-/-}$ and *ClpP*$^{+/-}$ mice obtained by mass spectrometry (n = 5).

(B) Left panels: Immunoblots of sWAT and BAT extracts from WT and *ClpP*$^{-/-}$ mice for Lon, Hsp60, Hsp40, ClpX, ClpP and β-tubulin/β-actin (n = 4-5). Right panels: graphical representation of quantified blots normalized to β-tubulin/β-actin.

(C) Left panels: Immunoblots of gWAT extracts from WT and *ClpP*$^{-/-}$ mice for PINK1, Parkin and β-actin. Right panels: graphical representation of quantified blots normalized to β-actin (n = 4).

Data information: (A-C) Bars represent mean ± SEM. (ANOVA, *WT/Control vs *ClpP*$^{-/-}$ /ClpPKD; #*ClpP*$^{+/-}$ vs *ClpP*$^{-/-}$. */#p<0.05). WT-white bars, *ClpP*$^{+/-}$-grey bars, *ClpP*$^{-/-}$-black bars.

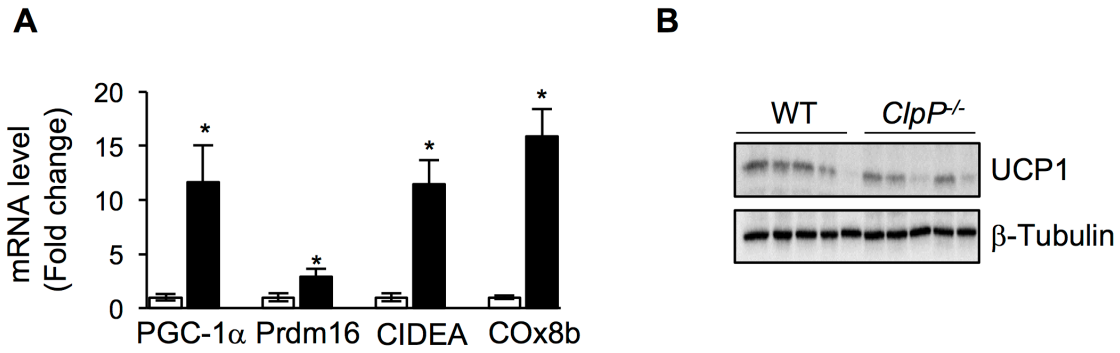

Appendix Figure S3. Absence of ClpP increases whole body energy expenditure, mitochondrial uncoupling and alters expression of metabolic enzymes in gWAT.

(A) Transcript levels of PGC-1α, Prdm16, CIDEA and Cox8b in sWAT, normalized to β-microglobulin (n = 6).
(B) Immunoblots of BAT extracts from WT and *ClpP*$^{-/-}$ mice for UCP1 and β-actin (n = 5).

Data information: (A, B) Bars represent mean ± SEM. (ANOVA, *WT/Control vs *ClpP,* *p<0.05). WT-white bars, *ClpP*$^{-/-}$-black bars.

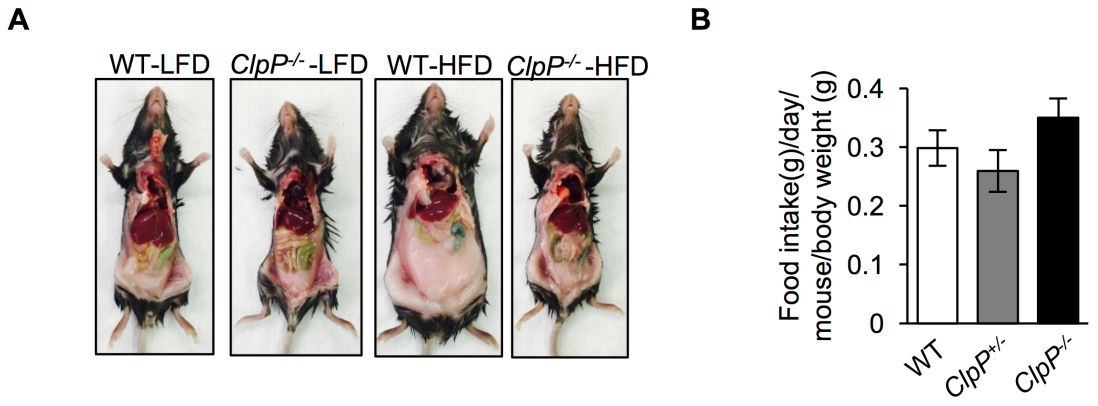

Appendix Figure S4. *ClpP*$^{-/-}$ mice are resistant to diet-induced obesity.

(A) Representative images of WT and *ClpP*$^{-/-}$ mice after 10-weeks of LFD or HFD-feeding.
(B) Food consumption of WT, *ClpP*$^{+/-}$ and *ClpP*$^{-/-}$ mice fed HFD, normalized to body weight. WT-white bars, *ClpP*$^{+/-}$-grey bars, *ClpP*$^{-/-}$-black bars (*n* =8-10).

Data information: (B) Bars represent mean ± SEM.